

Experimental validation of single-iteration multigrid wavefront reconstruction at the Palomar Observatory

Laurent Lessard,^{1,*} Douglas MacMynowski,² Matthew West,³ Antonin Bouchez,⁴ and Sanjay Lall¹

¹Department of Aeronautics and Astronautics, Stanford University, Durand Building, 496 Lomita Mall, Stanford, California 94305, USA

²Department of Control and Dynamical Systems, California Institute of Technology, 1200 East California Boulevard, Pasadena, California 91125, USA

³Department of Mechanical Science and Engineering, University of Illinois at Urbana-Champaign, 1206 West Green Street, Urbana, Illinois 61801, USA

⁴Caltech Optical Observatories, California Institute of Technology, 1200 East California Boulevard, Pasadena, California 91125, USA

*Corresponding author: lessard@stanford.edu

Received June 10, 2008; revised July 30, 2008; accepted August 1, 2008; posted August 7, 2008 (Doc. ID 97266); published September 8, 2008

Single-iteration multigrid (SIMG) wavefront reconstruction schemes were implemented and validated on the adaptive optics system at the Hale 5.1 m telescope at the Palomar Observatory. Results indicate that even the simplest such method produces a performance indistinguishable from that of the standard least-squares reconstructor for both bright and dim guide stars. SIMG provides a dramatic reduction in computational cost when compared to vector-matrix multiplication and can be implemented in parallel, making it the obvious choice for reconstruction in future large-scale adaptive optics systems. © 2008 Optical Society of America

OCIS codes: 010.1080, 010.7350, 350.1260.

Wavefront reconstruction is implemented on existing adaptive optics (AO) systems using vector-matrix multiplication (VMM). This is inadequate for future large (10^4 – 10^5 actuator) systems, since computation scales as $\mathcal{O}(n^2)$, where n is the number of actuators. Many faster methods have been proposed and analyzed using computer simulations. Examples include the conjugate-gradient (CG) [1], Fourier-domain (FD) [2], blended FD-CG [3], and sparse methods [4]. Recently, it was shown through simulation that a single-iteration multigrid (SIMG) method is as effective as CG methods for both multiconjugate [5] and single-conjugate adaptive optics (MCAO and SCAO, respectively) [6]. In this Letter, we detail the experimental validation of this work on a real SCAO system.

Two computationally efficient methods that have previously been tested on-sky are the FD method [7] and a sparse method [4]. These methods are $\mathcal{O}(n \log n)$. The SIMG is $\mathcal{O}(n)$ and shows no performance degradation when compared to the least-squares reconstructor.

A good model for the wavefront sensor (WFS) is [6,8]

$$y = Gx + v,$$

where x is the wavefront phase, y are the measurements, v is white noise, and G is a sparse influence matrix. The least-squares reconstruction matrix is found by taking the pseudoinverse. In practice, we can compute it by evaluating $K = (G^T G + \epsilon I)^{-1} G^T$ for a small ϵ . This ensures that unobservable modes such as piston and waffle are zeroed out. The SIMG method [6] uses a single multigrid sweep with an ini-

tial guess of 0 to obtain an approximate solution to the equation

$$(G^T G + \epsilon I) \hat{x} = (G^T y).$$

If the measurements are taken in open-loop, \hat{x} is the wavefront phase. In this case, $\hat{x}_0 = 0$ is a bad guess, so multiple iterations are required to achieve acceptable convergence [6]. However, when we operate in closed-loop, \hat{x} is the *change* in wavefront phase between successive time steps, and only one iteration is required.

Our tests were performed on the Palomar Adaptive Optics (PALAO) system on the Hale 5.1 m telescope [9]. The PALAO system has a deformable mirror (DM) with 241 active actuators and a Shack-Hartmann WFS array with 256 subapertures, producing a total of 512 measurements. The DM and WFS are aligned in a Fried geometry.

The AO system collects measurements y at up to 2 kHz. Tip and tilt are removed from the wavefront using a fast-steering mirror (FSM) and proportional-integral (PI) controller. The rest of the wavefront offset \hat{x} is reconstructed by VMM: $\hat{x} = Ky$. This estimate is fed back through a second PI loop to the DM. The closed-loop corrected wavefront is split using a dichroic mirror. The near-infrared portion is sent to the Palomar High Angle Resolution Observer (PHARO) [10]. See Fig. 1.

To implement the SIMG on the PALAO system, *virtual* actuators were added to fill the 17×17 grid containing the circular actuator arrangement, and the influence matrix G was augmented with zeros appropriately, as in [3]. The new system is $y = \bar{G}\bar{x}$, where \bar{G} is 512×289 instead of 512×241 . This new system is

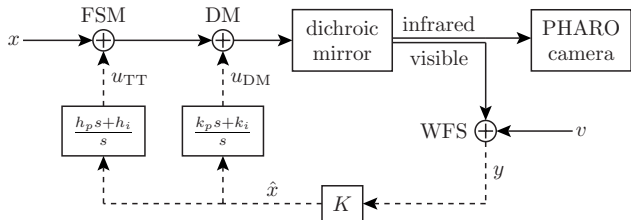


Fig. 1. Block diagram representing the PALAO system. Solid lines indicate the optical path, while dashed lines indicate the signal path. Note that the fast-steering mirror mirror (FSM), deformable mirror (DM), and wavefront sensor (WFS) are represented as summation junctions.

equivalent to the original one, so no approximation was made. We can now use the SIMG method [6] on this system and truncate the resulting \bar{x} to obtain x . It is worth noting that this simple trick destroys the *block-toeplitz with toeplitz block* structure of $G^T G$. Although this does not affect the SIMG in any way, methods such as FD reconstruction [2] or Fourier-based preconditioning [11] rely on a shift-invariant structure. To adapt to a circular aperture they must either use a heuristic to correct for edge effects [2] or use an enlarged computational domain [1,11]. No special provisions were made to account for the central obscured region; these measurements are simply zeroed.

For ease of testing we implemented the SIMG using the equivalent VMM reconstructor. Such a representation is possible, since the SIMG is a sequence of linear operations: Jacobi or Gauss–Seidel iterations, restriction–prolongation, residual computation, and multiplication by G^T . While this does not allow us to benefit from a computational speedup, it allows rapid sequential testing of different algorithms. The same approach was used in [4,7]. The 3217 actuator PALM-3000 system currently in development [12] is being designed with sufficient computation to allow full VMM reconstructors; this will permit similar experiments on a much larger system to be conducted in the future.

On May 19, 2008, we ran tests on three stars that ranged from bright (magnitude 8) to dim (magnitude 13.5). The sky was exceptionally calm and clear during our experiment, so we chose a very dim star for our final test. For each star, we adjusted the WFS sample rate, tip–tilt control gains, and DM control gains to maximize the Strehl ratio using the baseline (least-squares) reconstructor; see Table 1. The signal-to-noise ratio (SNR) per subaperture was measured by comparing the average flux per subaperture to the variance while the WFS was recording the sky background frames [8]. We used a Kshort filter

(1.99 to 2.30 μm) plus a neutral density filter appropriate for the star brightness: 0.1% for the two brighter stars, and no filter for the faintest star.

We tested the baseline least-squares reconstructor and three multigrid schemes. One of them was GS(1,0)-V, meaning we used a Gauss–Seidel smoother in a V cycle, with one presmoothing iteration and no postsmoothing. The other two were GS(1,1)-V, and J(1,0)-V, where the J indicates a Jacobi smoother. Each V cycle is run only once per measurement. Note that J(1,0)-V is the simplest possible multigrid method. More complicated variations such as GS(2,2)-W using a W cycle are also possible. Alternatively, one can execute multiple iterations of a chosen method per measurement. In the limit, these more complicated (and costlier) variations approach the baseline least-squares reconstructor. In our experiment, we tested the three simplest reconstructors

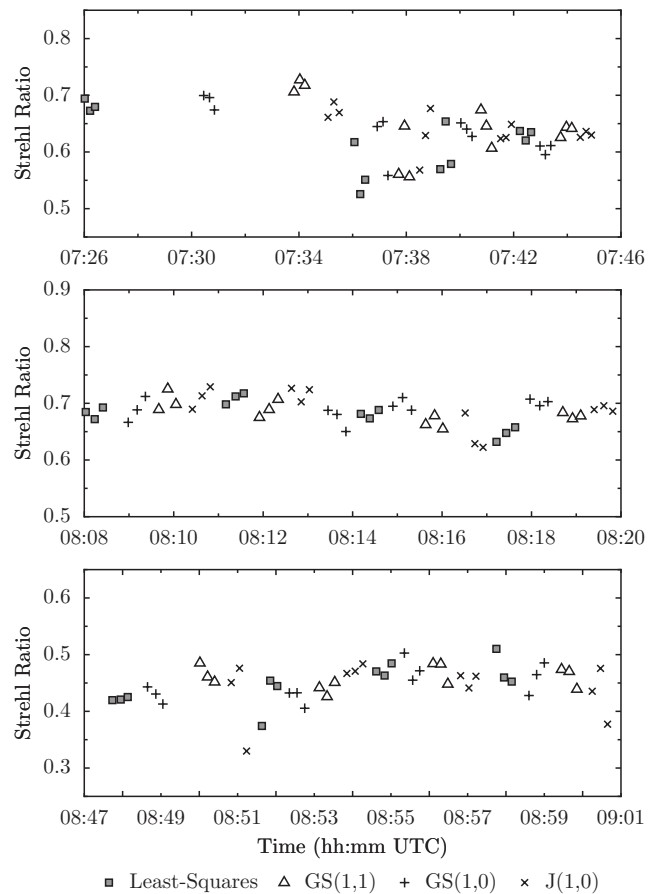


Fig. 2. Plot comparing the Strehl ratio of various reconstructors on Stars 1, 2, and 3 (top, middle, and bottom, respectively). Each point represents a 10 s exposure image.

Table 1. System Parameters Used for Each Star^a

Number	Catalog Designation	Brightness	Sample Rate	Tip–Tilt gain	SNR
1	Tycho-2 2563-170-1	$V=8.10$	1 kHz	0.30	14.9
2	Tycho-2 2580-2328-1	$V=10.01$	500 Hz	0.40	11.8
3	USNO-B1.0 1204-0241816	$R=13.5$	50 Hz	0.40	3.5

^aThe sample rates and tip–tilt integral gains above were chosen to optimize the instantaneous Strehl ratio. The optimal DM gains were the same for each star: a proportional gain of 0.25 and an integral gain of 0.01.

and found that their performance was indistinguishable from that of the baseline least-squares reconstructor.

Each reconstructor was tested four times per star, and each test consisted of acquiring three consecutive 10 s exposure images. This cyclical testing pattern allows us to average performance over the variable atmospheric conditions and was inspired by a similar experiment to test a Fourier-based reconstructor at Palomar [7]. We also collected images of the sky background by pointing the telescope 60 arc sec away from the target star, before and after the reconstructors were tested.

For each image we computed the Strehl ratio by first subtracting the median sky background from each frame (eliminating sky photons and detector bias). We then measured the ratio of the peak brightness of the star to that of a theoretical diffraction-limited point-spread function with the same total flux and pixel position. Refer to Fig. 2 for plots showing the Strehl ratio for three stars. The gaps in time during the first test are owing to restarting the AO system. The four methods tested performed equally well. This agrees with recent theoretical predictions [6].

The seeing measured by the combined Multi-Aperture Scintillation Sensor (MASS)–Differential Image Motion Monitor (DIMM) instrument at the Palomar Observatory [13] is plotted over the time of this experiment in Fig. 3. The higher variability in Strehl ratio measured for stars 1 and 3 is consistent with the observed variability in seeing. The average and Strehl ratio for each method is compared for the second star in Fig. 4. These data have the lowest variance, so if there is any appreciable difference between the methods, it would show up here.

This experiment has shown that SIMG methods perform as well as least-squares reconstruction on a real AO system for both bright and dim guide stars. The major benefit of using SIMG is reduced computation. A system with n actuators yields roughly $2n$ sensor measurements, and therefore, $2n^2$ multiplications per time step are required to process the measurements using VMM. In contrast, about $27n$ are required for MG-J(1,0)-V or MG-GS(1,0)-V, and $34n$ for MG-GS(1,1)-V. This includes the multiplication by G^T and the cost of smoothing, residual computation, restriction, and prolongation on every level. For the PALAO system, this results in fewer multiplications

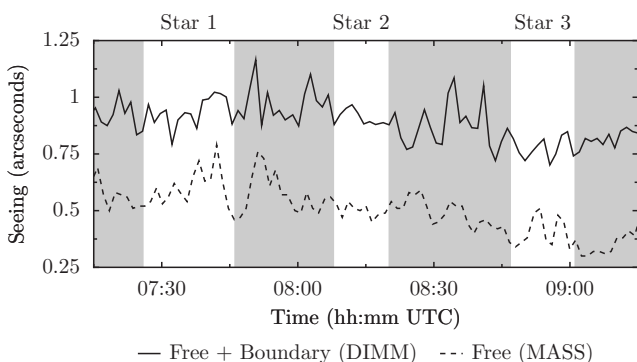


Fig. 3. MASS-DIMM seeing at 500 nm measured throughout the night.

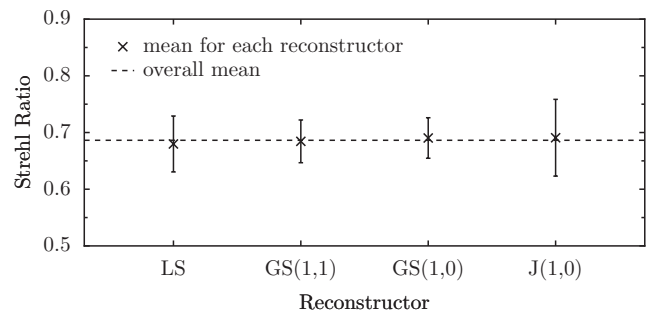


Fig. 4. Plot showing the mean performance of each reconstructor on Star 2. The error bars indicate the 95% confidence interval for the true mean. There is no statistically discernable difference in performance between the four reconstructors we tested. The two other stars have similar plots, but with higher variances.

by a factor of about 17.

For a 3217 actuator system such as the PALM-3000 [12], using SIMG would reduce reconstruction computation by a factor of about 220 compared to VMM. Furthermore, if we use a Jacobi smoother, every step of the reconstruction is highly parallelizable; even if the sensor measurements are read sequentially, we can perform all the fine-grid computations, or roughly 3/4 of the work, while the data are being read in. Recent theoretical simulations of SIMG for the SCAO [6] and MCAO cases [5] show that these methods scale well to extremely large systems, making SIMG the obvious choice for current and future large AO systems.

References

1. L. Gilles, C. R. Vogel, and B. L. Ellerbroek, *J. Opt. Soc. Am. A* **19**, 1817 (2002).
2. L. A. Poyneer, D. T. Gavel, and J. M. Brase, *J. Opt. Soc. Am. A* **19**, 2100 (2002).
3. H. Ren, R. Dekany, and M. Britton, *Appl. Opt.* **44**, 2626 (2005).
4. F. Shi, D. G. MacMartin, M. Troy, G. L. Brack, R. S. Burruss, and R. G. Dekany, *Proc. SPIE* **4839**, 1035 (2003).
5. L. Gilles, B. Ellerbroek, and C. Vogel, in *Adaptive Optics: Analysis and Methods/Computational Optical Sensing and Imaging/Information Photonics/Signal Recovery and Synthesis Topical Meetings on CD-ROM* (Optical Society of America, 2007), paper JTua1.
6. L. Lessard, M. West, D. MacMynowski, and S. Lall, *J. Opt. Soc. Am. A* **25**, 1147 (2008).
7. L. A. Poyneer, M. Troy, B. Macintosh, and D. Gavel, *Opt. Lett.* **28**, 798 (2003).
8. J. W. Hardy, *Adaptive Optics for Astronomical Telescopes* (Oxford U. Press, 1998).
9. M. Troy, R. G. Dekany, G. Brack, B. R. Oppenheimer, E. E. Bloemhof, T. Trinh, F. G. Dekens, F. Shi, T. L. Hayward, and B. Brandl, *Proc. SPIE* **4007**, 31 (2000).
10. T. L. Hayward, B. Brandl, B. Pirger, C. Blacken, G. E. Gull, J. Schoenwald, and J. R. Houck, *Publ. Astron. Soc. Pac.* **113**, 105 (2001).
11. Q. Yang, C. R. Vogel, and B. L. Ellerbroek, *Appl. Opt.* **45**, 5281 (2006).
12. R. Dekany, A. Bouchez, M. Britton, V. Velur, M. Troy, J. C. Shelton, and J. Roberts, *Proc. SPIE* **6272**, 62720G (2006).
13. V. Kornilov, A. Tokovinin, N. Shatsky, O. Voziakova, S. Potanin, and B. Safonov, *Mon. Not. R. Astron. Soc.* **382**, 1268 (2007).